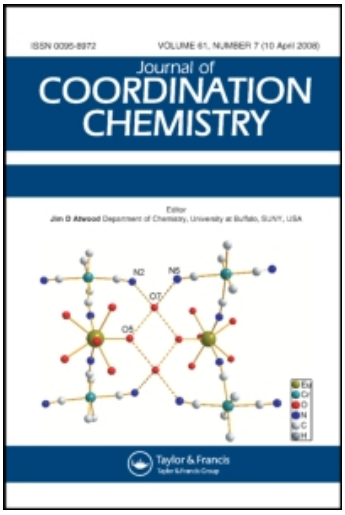


**Journal of Coordination Chemistry**
Publication details, including instructions for authors and subscription information:
http://www.informaworld.com/smpp/title~content=t713455674

# Heat-induced changes in microstructure and magnetic properties of $Co_{0.75}Ni_{0.75}[Fe(CN)_6] \cdot XH_2O$

Li Liu[a]; Min Liu[a]; Xiaofang Bian[a]; Haosheng Wu[a]; Mingxiang Xu[a]
[a] Department of Physics, Southeast University, Nanjing 210096, China

First published on: 06 October 2010

**To cite this Article** Liu, Li , Liu, Min , Bian, Xiaofang , Wu, Haosheng and Xu, Mingxiang(2010) 'Heat-induced changes in microstructure and magnetic properties of $Co_{0.75}Ni_{0.75}[Fe(CN)_6] \cdot XH_2O$', Journal of Coordination Chemistry, 63: 22, 3907 — 3913, First published on: 06 October 2010 (iFirst)
**To link to this Article: DOI:** 10.1080/00958972.2010.522706
**URL:** http://dx.doi.org/10.1080/00958972.2010.522706

*Journal of Coordination Chemistry*
Vol. 63, No. 22, 20 November 2010, 3907–3913



# Heat-induced changes in microstructure and magnetic properties of $Co_{0.75}Ni_{0.75}[Fe(CN)_6] \cdot XH_2O$

LI LIU*, MIN LIU, XIAOFANG BIAN, HAOSHENG WU and MINGXIANG XU*

Department of Physics, Southeast University, Nanjing 210096, China

(*Received 13 March 2010; in final form 2 August 2010*)



Polycrystalline $Co_{0.75}Ni_{0.75}[Fe(CN)_6] \cdot XH_2O$ was prepared by coprecipitation. The coprecipitated powder was annealed in vacuum at 80°C, 100°C, and 130°C. Variation of microstructural and magnetic properties with different annealed temperatures was studied by Fourier-transform infrared, X-ray diffraction, and magnetization measurements. The differences in magnetic phase transition temperature, coercivity, remanence, and effective magnetization were studied in detail. The magnetic contribution mainly results from $Fe^{III}$–CN–$Co^{II}/Ni^{II}$ and $Fe^{III}$–NC–$Co^{II}/Ni^{II}$ because $Fe^{II}$–CN–$Co^{III}/Ni^{II}$ carries no net spin. After annealing at 130°C, the microstructures $Fe^{III}$–CN–$Co^{II}/Ni^{II}$ and $Fe^{III}$–NC–$Co^{II}/Ni^{II}$ convert to $Fe^{II}$–CN–$Co^{III}/Ni^{II}$. Differences in magnetic properties may be attributed to heat-induced microstructural changes.

*Keywords*: Annealing temperature; Infrared spectroscopy; Microstructural changes; Magnetic properties

## 1. Introduction

Design of materials with high critical temperatures has been a challenge in molecular materials [1–5], to improve magnetic properties and achieve unusual properties, such as photomagnetic effect [6–10], thermal–magnetic effect [10, 11] and spin-glass behavior [12–16]. Heat treatment has been accompanied by dramatic physical property changes in Prussian blue analogs [16–20]. Promising results in $M_{1.5}[Fe(CN)_6] \cdot XH_2O$ (M = Ni, Co, Cu, and Zn) have been observed [18–20]. The fraction of the electronic states in $Co_3[Fe(CN)_6]_2 \cdot XH_2O$ is sensitive to anneal temperature, which induces a charge transfer from $Co^{II}$ to $Fe^{III}$ [19, 20], increasing the fraction of $Fe^{II}$–CN–$Co^{III}$, paramagnetic even at low temperature. Kumar *et al.* [13, 15] reported the structural and magnetic properties of $Co_xNi_{1-x}[Fe(CN)_6] \cdot ZH_2O$ annealed under an infrared (IR) lamp. Their study highlighted the importance in designing molecular magnets with varying magnetic properties of Prussian blue analogs. However, magnetic properties with different anneal temperatures in $Co_{0.75}Ni_{0.75}[Fe(CN)_6] \cdot XH_2O$ has not been previously studied. Magnetic properties influenced by heating $Co_{0.75}Ni_{0.75}[Fe(CN)_6] \cdot XH_2O$ will be essential from a fundamental point of view and are vital for further practical

*Corresponding authors. Email: liuli1101@126.com; mxxu@seu.edu.cn

*Journal of Coordination Chemistry*
ISSN 0095-8972 print/ISSN 1029-0389 online © 2010 Taylor & Francis
DOI: 10.1080/00958972.2010.522706

studies. In this study, microstructures and variation of magnetic properties with different anneal temperatures were systematically studied from elemental analysis, IR spectroscopy, X-ray diffraction (XRD), and magnetization measurements.

## 2. Experimental

Polycrystalline $Co_{0.75}Ni_{0.75}[Fe(CN)_6]\cdot XH_2O$ was prepared by coprecipitation from mixed aqueous solutions of (50 mL, 4.15 mmol) $Co(NO_3)_2\cdot 6H_2O$ and (50 mL, 4.15 mmol) $Ni(NO_3)_2\cdot 6H_2O$ poured into aqueous solution of (100 mL, 4.15 mmol) $K_3[Fe(CN)_6]$. An excess of $Co^{2+}$ and $Ni^{2+}$ to $[Fe(CN)_6]^{3+}$ (ratio = 2 : 1) was used to make potassium-free precipitates. After a powder formed, the resulting powder was filtered, washed several times with doubly distilled water, and finally dried in a vacuum oven at 80°C, 100°C, or 130°C for 24 h [15].

Elemental analysis (Perkin Elmer Corporation PE2400 II), Fourier transform infrared (FT-IR) spectroscopy (Perkin Elmer Corporation PE Spectrum One FT-IR spectrometer, KBr pellet) from 400–4000 $cm^{-1}$, and powder XRD (Siemens XRD 5500) using Cu-K$\alpha$ radiation were used to characterize the samples. Magnetization was measured by a vibrating sample magnetometer (VSM) integrated in a physical property measurement system (PPMS-9, Quantum Design) up to 70,000 Oe from 2 to 300 K.



## 3. Results and discussion

### 3.1. *Elemental analysis*

From elemental analysis, the powder annealed at 80°C has a chemical composition of $Co_{0.75}Ni_{0.75}[Fe(CN)_6]\cdot 6.1H_2O$. Anal. Calcd for $Co_{0.75}Ni_{0.75}[Fe(CN)_6]\cdot 6.1H_2O$: C, 17.57; H, 3.00; N, 20.49. Found: C, 17.7; H, 2.96; N, 20.2. The powder annealed at 100°C has a chemical composition of $Co_{0.75}Ni_{0.75}[Fe(CN)_6]\cdot 5H_2O$. Anal. Calcd for $Co_{0.75}Ni_{0.75}[Fe(CN)_6]\cdot 5H_2O$: C, 18.47; H, 2.58; N, 21.54. Found: C, 18.7; H, 2.53; N, 21.6. The powder annealed at 130°C has a chemical composition of $Co_{0.75}Ni_{0.75}[Fe(CN)_6]\cdot 5H_2O$. Anal. Calcd for $Co_{0.75}Ni_{0.75}[Fe(CN)_6]\cdot 5H_2O$: C, 18.47; H, 2.58; N, 21.54. Found: C, 18.5; H, 2.55; N, 21.4.

### 3.2. *FT-IR spectroscopy*

Figure 1 shows FT-IR spectra of $Co_{0.75}Ni_{0.75}[Fe(CN)_6]\cdot XH_2O$ annealed at 80°C, 100°C, and 130°C. FT-IR spectra of cyano complexes have been studied extensively [17, 18], easily identified since they exhibit sharp $\nu$(CN) at 2000–2200 $cm^{-1}$. Room temperature IR and Mössbauer spectroscopies give evidence of two $Fe^{III}$ sites in $Co_{0.75}Ni_{0.75}[Fe(CN)_6]\cdot 6.8H_2O$ annealed under an IR lamp [13, 15]. The $Fe^{III}$–NC–$Co^{II}/Ni^{II}$ structure may be due to heating of the sample; similar results have been reported for $Cu_{1.5}[Fe(CN)_6]\cdot 6H_2O$ [21], and $K_{0.2}Co_{1.4}[Fe(CN)_6]\cdot 7H_2O$ [19]. The flipping of cyanide is evident from the structural refinement [13, 19, 21]. $Fe^{III}$ in $Fe^{III}$–CN–$Co^{II}/Ni^{II}$ is low spin ($S = 1/2$) and $Fe^{III}$ in $Fe^{III}$–NC–$Co^{II}/Ni^{II}$ is

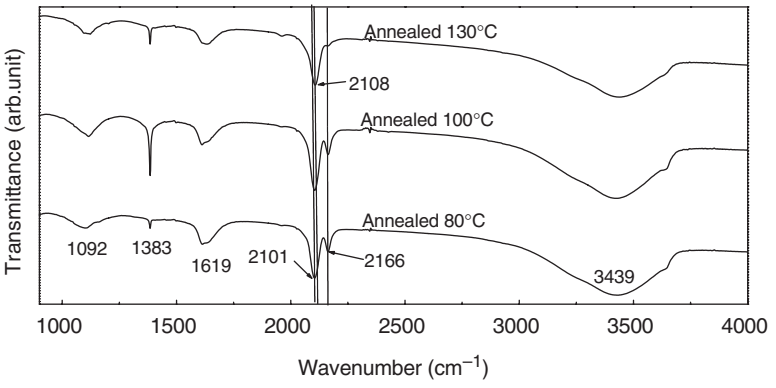


Figure 1. FT-IR spectra of $Co_{0.75}Ni_{0.75}[Fe(CN)_6] \cdot XH_2O$ annealed at 80°C, 100°C, and 130°C.



high spin ($S = 5/2$) [13]. Anneal temperatures above 80°C induce a charge transfer from $Co^{II}$ to $Fe^{III}$ in $Co_3[Fe(CN)_6]_2 \cdot XH_2O$ [8, 19, 20]. According to Mössbauer results, the charge transfer leads to reduction in the amount of $Fe^{III}$ and $Co^{II}$ to form low-spin $Fe^{II}$ ($S = 0$) and $Co^{III}$ [20]. $Co_{0.75}Ni_{0.75}[Fe(CN)_6] \cdot XH_2O$ annealed at 80°C, 100°C, and 130°C are characterized by three peaks, 2101, 2108, and 2166 $cm^{-1}$, which can be assigned to $\nu(Fe^{III}–NC–Co^{II}/Ni^{II})$, $\nu(Fe^{II}–CN–Co^{III})$, and $\nu(Fe^{III}–CN–Co^{II}/Ni^{II})$, respectively [13, 20]. The formal expression for $\nu$(CN) energy is $U(0) = 1/2\,h\nu$, where $h$ is the Plank constant and $\nu$ is the vibration frequency. The $\nu$(CN) energies at 2101, 2108 and 2166 $cm^{-1}$ are 12.576, 12.620, and 12.968 KJ $mol^{-1}$, respectively. The energy difference of $\nu$(CN) from $Fe^{III}–NC–Co^{II}$ to $Fe^{II}–CN–Co^{III}$ is 0.044 KJ $mol^{-1}$. The thermal energy of $\nu$(CN) is $E = 1/2\,K_BT$, where $K_B$ is the Boltzmann constant and $T$ is the temperature. According to the calculation, the thermal energy difference is $4.1538\Delta T$ J $mol^{-1}$, bigger than the energy difference of the $\nu$(CN) from $Fe^{III}–NC–Co^{II}$ to $Fe^{II}–CN–Co^{III}$. Heating can induce charge transfer from $Co^{II}$ to $Fe^{III}$. As annealing temperature is increased, intensity of the peak at 2108 $cm^{-1}$ increases and decreases at the peaks 2101 and 2166 $cm^{-1}$. After annealing at 130°C, the microstructures of $Fe^{III}–CN–Co^{II}/Ni^{II}$ and $Fe^{III}–NC–Co^{II}/Ni^{II}$ convert to $Fe^{II}–CN–Co^{III}$. Broad peak at 3439 $cm^{-1}$ and peak at 1619 $cm^{-1}$ correspond to $\nu$(O–H) of the crystal water.

### 3.3. *Powder XRD*

XRD profiles of $Co_{0.75}Ni_{0.75}[Fe(CN)_6] \cdot XH_2O$ annealed at 80°C, 100°C, and 130°C are provided in "Supplementary material" and physical parameters are listed in table 1. All diffraction peaks can be identified with NaCl-type structure with space group *Fm*3*m*. The line broadening and positions found in the XRD peaks are the same between the three samples. The lattice parameters decrease slightly from 10.2383 to 10.2340 Å with an increase in annealing temperature from 80°C to 130°C. This corresponds to cell contraction related to the charge transfer, a shorter $Fe^{III}–NC–Co^{II}/Ni^{II}–CN–Fe^{III}$ chain length. With higher amount of Co(III) ferrocyanide formed, contribution to that cell contraction is also due to formation of low-spin Fe(II), which means a smaller Fe–C distance by stronger $\pi$-back bonding interaction with CN [20]. The small dependence of

Table 1. Summary of physical parameters for $Co_{0.75}Ni_{0.75}[Fe(CN)_6]\cdot XH_2O$ annealed at different temperatures.

| Treatment | Lattice parameter $a_0$ (Å) | Unit cell volume $a_0^3$ (Å$^3$) |
|---|---|---|
| Annealed at 80°C | 10.238(3) | 1073.2(0) |
| Annealed at 100°C | 10.234(8) | 1072.1(0) |
| Annealed at 130°C | 10.234(0) | 1071.8(5) |

lattice parameter on the annealing temperature implies that no structural changes are involved in the samples.

### 3.4. *Direct current magnetization*

Magnetic interactions in the cyanide complex are superexchange interactions *via* CN bridges. These interactions may be positive ferromagnetic, negative antiferromagnetic, or ferromagnetic depending upon the symmetries of the magnetic orbitals involved. Superexchange interactions between orthogonal orbitals (e.g., $t_{2g}$ and $e_g$) favor a ferromagnetic ordering whereas superexchange interactions between same symmetry orbitals (e.g., $t_{2g}$ and $t_{2g}$, and $e_g$ and $e_g$) are antiferromagnetic [19, 20]. IR results have shown the presence of noninteracting $Fe^{II}$–CN–$Co^{III}$, $Fe^{III}$–NC–$Co^{II}$/$Ni^{II}$, and $Fe^{III}$–CN–$Co^{II}$/$Ni^{II}$ linear chains in the compounds. By considering the symmetry of various magnetic orbitals, one can see that the magnetic interactions between $Ni^{II}$ $t_{2g}^6e_g^2$ ($S=1$) and low-spin $Fe^{III}$ $t_{2g}^6e_g^2$ ($S=1/2$) will be ferromagnetic. However, for magnetic interactions between high-spin $Co^{II}$ $t_{2g}^5e_g^2$ ($S=3/2$) and low-spin $Fe^{III}$ $t_{2g}^6e_g^2$ ($S=1/2$), both ferromagnetic and antiferromagnetic interaction are present, but overall, the ferromagnetic interaction is dominant. In the case of magnetic interactions between high-spin $Co^{II}$ $t_{2g}^5e_g^2$ ($S=3/2$) and low-spin $Fe^{III}$ $t_{2g}^6e_g^2$ ($S=1/2$), the ferromagnetic interaction is dominant. For magnetic interactions between high-spin $Fe^{III}$ $t_{2g}^6e_g^2$ ($S=5/2$) and low-spin $Co^{II}$ $t_{2g}^6e_g^1$ ($S=1/2$), the ferromagnetic interaction is dominant. Ferromagnetic interaction between $Ni^{II}$ $t_{2g}^6e_g^2$ ($S=1$) and high-spin $Fe^{III}$ $t_{2g}^3e_g^2$ ($S=5/2$) is dominant [20]. In the microstructure $Fe^{II}$–CN–$Co^{III}$/$Ni^{II}$, $Fe^{II}$ ($S=0$) is diamagnetic and magnetic contribution from $Fe^{II}$–CN–$Co^{III}$/$Ni^{II}$ species must be very weak. So, the model of superexchange interactions indicates a predominant ferromagnetic interaction over the antiferromagnetic in this compound [22].

Field-cooled (FC) and zero field-cooled (ZFC) magnetization curves at 200 Oe field are shown in figure 2. A clear branching between the FC and ZFC magnetization curves is evident. The ZFC curves rise slowly till the temperature is lowered from 300 to 18 K, after that it shoots up sharply showing maximum (around 9.4 K for $Co_{0.75}Ni_{0.75}[Fe(CN)_6]\cdot 6.1H_2O$ annealed at 80°C, 9.4 K for $Co_{0.75}Ni_{0.75}[Fe(CN)_6]\cdot 5H_2O$ annealed at 100°C and 8.2 K for $Co_{0.75}Ni_{0.75}[Fe(CN)_6]\cdot 5H_2O$ annealed at 130°C) and decreases as temperature is decreased further. This behavior is characteristic of spin-glass state. The variation of branching temperature, $T_{irr}$ (temperature below which FC and ZFC magnetization curves separates), and $T_{max}$ (temperature at which a peak in ZFC magnetization is found) decrease with anneal temperature increase from 100°C to 130°C.

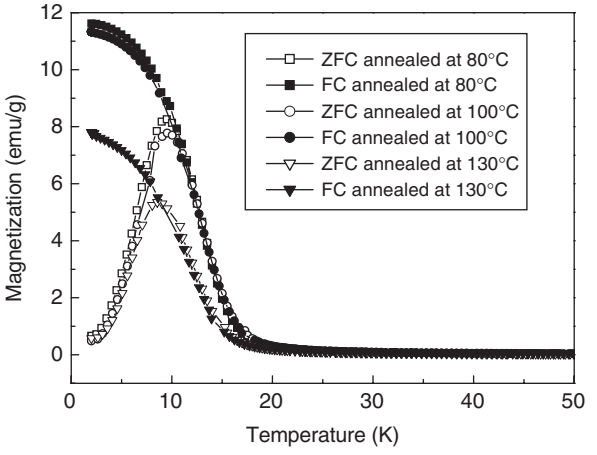


Figure 2. FC and ZFC magnetization curves at 200 Oe of $Co_{0.75}Ni_{0.75}[Fe(CN)_6] \cdot XH_2O$ annealed at 80°C, 100°C, and 130°C.



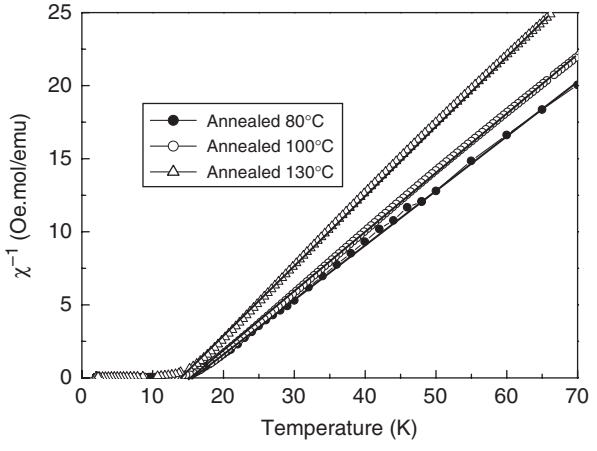


Figure 3. Temperature dependence of $\chi^{-1}$ curves of $Co_{0.75}Ni_{0.75}[Fe(CN)_6] \cdot XH_2O$ annealed at 80°C, 100°C, and 130°C.

Figure 3 shows temperature dependence of $\chi^{-1}$ in the temperature range 2–70 K. Straight line is fit to data from 16 to 70 K. The Curie constant, C, and Curie–Weiss temperature, $\theta$, are determined from a linear fitting of $1/\chi = (T-\theta)/C$ (Curie–Weiss law) to the linear region, giving $C = 2.697\,\text{emu K/(mol} \cdot \text{Oe)}$, paramagnetic Curie temperature $\theta = 15.6\,\text{K}$ for annealing at 80°C, $C = 2.521\,\text{emu K/(mol} \cdot \text{Oe)}$, $\theta = 15.3\,\text{K}$ for annealing at 100°C, and $C = 2.115\,\text{emu K/(mol} \cdot \text{Oe)}$, and $\theta = 13.7\,\text{K}$ for annealing at 130°C. The effective paramagnetic moments, $\mu_{\text{eff}} = (3CK_B/N_A\mu_B^2)^{1/2} \approx (8C)^{1/2}$, are 4.645, 4.491, and 4.113 for $Co_{0.75}Ni_{0.75}[Fe(CN)_6] \cdot XH_2O$ annealed at 80°C, 100°C, and 130°C, respectively, decrease with the increase in annealing temperature. According to the IR results, $Fe^{III}$–CN–$Co^{II}/Ni^{II}$ and $Fe^{III}$–NC–$Co^{II}/Ni^{II}$ can convert

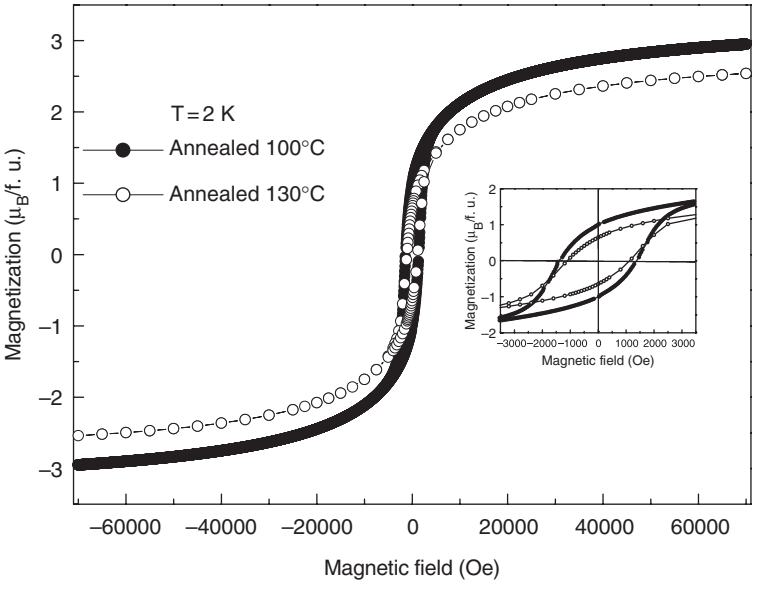


Figure 4. Hysteresis curves at 2 K for $Co_{0.75}Ni_{0.75}[Fe(CN)_6] \cdot XH_2O$ annealed at 100°C and 130°C. The inset shows enlarged curves between −3500 and 3500 Oe.



to $Fe^{II}$–CN–$Co^{III}/Ni^{II}$ after annealing at 130°C. The magnetic contribution mainly results from $Fe^{III}$–CN–$Co^{II}/Ni^{II}$ and $Fe^{III}$–NC–$Co^{II}/Ni^{II}$ because $Fe^{II}$–CN–$Co^{III}/Ni^{II}$ carries no net spin. So changes of the effective paramagnetic moment may be attributed to heat-induced microstructural changes. The positive $\theta$ indicates a predominant ferromagnetic interaction in this compound [13].

Hysteresis curves at 2 K for a 70,000 Oe field are shown in figure 4. Hysteresis with a coercive field (see inset of figure 4) ($H_C$) of 1350 Oe and remanence of 0.984 $\mu_B$ f.u.$^{-1}$ for $Co_{0.75}Ni_{0.75}[Fe(CN)_6] \cdot 5H_2O$ annealed at 100°C, and a coercive field ($H_C$) of 1102 Oe, and remanence of 0.648 $\mu_B$ f.u.$^{-1}$ for $Co_{0.75}Ni_{0.75}[Fe(CN)_6] \cdot 5H_2O$ annealed at 130°C, are evident. The magnetic moments at 70,000 Oe field are 2.953 and 2.551 $\mu_B$ per formula unit for annealing at 100°C and 130°C, respectively. The values of coercive field and remanence decrease as the annealing temperature increases from 100°C to 130°C, explained by the amount of the $Fe^{II}$–CN–$Co^{III}/Ni^{II}$ relative to $Fe^{III}$–CN–$Co^{II}/Ni^{II}$ and $Fe^{III}$–NC–$Co^{II}/Ni^{II}$ increases with increased annealing temperature.

## 4. Conclusions

Molecular magnet $Co_{0.75}Ni_{0.75}[Fe(CN)_6] \cdot XH_2O$ has been prepared by coprecipitation. The resulting powder was dried in a vacuum oven at 80°C, 100°C, and 130°C. XRD measurements show that no structural changes are involved in the samples. FT-IR measurements show that microstructures $Fe^{III}$–NC–$Co^{II}/Ni^{II}$ and $Fe^{III}$–CN–$Co^{II}/Ni^{II}$ can convert to $Fe^{II}$–CN–$Co^{III}$ after annealing at 130°C. The magnetic phase transition temperature, coercivity, remanence, and effective magnetization with

anneal temperatures of 80°C, 100°C, and 130°C are different. The magnetic contribution results from $Fe^{III}$–CN–$Co^{II}/Ni^{II}$ and $Fe^{III}$–NC–$Co^{II}/Ni^{II}$ because $Fe^{II}$–CN–$Co^{III}/Ni^{II}$ carries no net spin. Differences in magnetic properties may be attributed to heat-induced microstructural changes.

## Acknowledgments

This study was partially supported by Foundation for Climax Talents Plan in Six-Big Fields of Jiangsu Province of China (Grant No. 1107020070), National Science Foundation of Jiangsu Province of China (Grant No. BK2010421), and Foundation for Undergraduate Innovative Experiment Plan of China (Grant No. 91028628).

## References



[1] S. Ferlay, T. Mallsah, R. Ouahes. *Nature*, **378**, 701 (1995).
[2] T. Mallah, S. Thiébaut, M. Verdaguer, P. Veillet. *Science*, **262**, 1554 (1993).
[3] O. Sato, T. Iyoda, A. Fujishima, K. Hashimoto. *Science*, **271**, 49 (1996).
[4] S.M. Holmes, A.S. Whelpley, G.S. Girolami. *Polyhedron*, **26**, 2291 (2007).
[5] R. Garde, J.M. Herrera, F. Villain, M. Verdaguer. *Inorg. Chim. Acta*, **361**, 3597 (2008).
[6] A. Goujon, F. Varret, V. Escax, A. Bleuzen, M. Verdaguer. *Polyhedron*, **20**, 1339 (2001).
[7] Z. Salman, T.J. Parolin, K.H. Chow, T.A. Keeler, R.I. Miller, D. Wang, J. Chakhalian, W.A. MacFarlane. *Physica B*, **374–375**, 130 (2006).
[8] D.A. Pejakovic, J.L. Manson, J.S. Miller, A.J. Epstein. *Curr. Appl. Phys.*, **1**, 15 (2001).
[9] S.I. Ohkoshi, H. Tokoro, K. Hashimoto. *Coord. Chem. Rev.*, **249**, 1830 (2005).
[10] O. Sato, T. Iyoda, A. Fujishima, K. Hashimoto. *Science*, **272**, 704 (1996).
[11] H. Tokoro, S.I. Ohkoshi, T. Matsuda, K. Hashimoto. *Inorg. Chem.*, **43**, 5231 (2004).
[12] H. Osawa, T. Iwazumi, H. Tokoro, S.I. Ohkoshi, K. Hashimoto, H. Shoji, E. Hirai, T. Nakamura, S. Nanaoa, Y. Isozumi. *Solid State Commun.*, **125**, 237 (2003).
[13] A. Kumar, S.M. Yusuf. *Physica B*, **362**, 278 (2005).
[14] W.E. Buschmann, J.S. Miller. *Inorg. Chem.*, **39**, 2411 (2000).
[15] A. Kumar, S.M. Yusuf, L. Keller, J.V. Yakhmi, J.K. Srivastava, P.L. Paulose. *Phys. Rev. B*, **75**, 224419 (2007).
[16] C.W. Ng, J. Ding, L. Wang, L.M. Gan, C.H. Quek. *J. Phys. Chem. A*, **104**, 8814 (2000).
[17] C.W. Ng, J. Ding, L.M. Gan. *J. Phys. D*, **34**, 1188 (2001).
[18] R. Martinez-Garcia, M. Knobel, E. Reguera. *J. Phys. Chem. B*, **110**, 7296 (2006).
[19] C.W. Ng, J. Ding, L.M. Gan. *J. Solid State Chem.*, **156**, 400 (2001).
[20] R. Martinez-Garcia, M. Knobel, G. Goya, M.C. Gimenez, F.M. Romero, E. Reguera. *J. Phys. Chem. Solids*, **67**, 2289 (2006).
[21] C.W. Ng, J. Ding, Y. Shi, L.M. Gan. *J. Phys. Chem. Solids*, **62**, 767 (2001).
[22] M. Verdaguer, A. Bleuzen, V. Marvaud, J. Vaissermann, M. Seuleiman, C. Desplanches, A. Scuiller, C. Train, R. Garde, G. Gelly, C. Lomenech, I. Rosenman, P. Veillet, C. Cartier, F. Villain. *Coord. Chem. Rev.*, **190–192**, 1023 (1999).